Hindawi Publishing Corporation
International Journal of Spectroscopy
Volume 2016, Article ID 7521050, 9 pages
http://dx.doi.org/10.1155/2016/7521050

Research Article

Electron Density from Balmer Series Hydrogen Lines and Ionization Temperatures in Inductively Coupled Argon Plasma Supplied by Aerosol and Volatile Species

Jolanta Borkowska-Burnecka, Wiesław Żyrnicki, Maja Wełna, and Piotr Jamróz

Chemistry Department, Division of Analytical Chemistry and Chemical Metallurgy, Wroclaw University of Technology, Wybrzeze Wyspianskiego 27, 50-370 Wroclaw, Poland

Correspondence should be addressed to Wiesław Żyrnicki; wieslaw.zyrnicki@pwr.edu.pl

Received 29 October 2015; Revised 15 February 2016; Accepted 1 March 2016

Academic Editor: Eugene Oks

Electron density and ionization temperatures were measured for inductively coupled argon plasma at atmospheric pressure. Different sample introduction systems were investigated. Samples containing Sn, Hg, Mg, and Fe and acidified with hydrochloric or acetic acids were introduced into plasma in the form of aerosol, gaseous mixture produced in the reaction of these solutions with $NaBH_4$ and the mixture of the aerosol and chemically generated gases. The electron densities measured from H_α, H_β, H_γ, and H_δ lines on the base of Stark broadening were compared. The study of the H Balmer series line profiles showed that the n_e values from H_γ and H_δ were well consistent with those obtained from H_β which was considered as a common standard line for spectroscopic measurement of electron density. The n_e values varied from $0.56 \cdot 10^{15}$ to $1.32 \cdot 10^{15}$ cm^{-3} and were the highest at loading mixture of chemically generated gases. The ionization temperatures of plasma, determined on the base of the Saha approach from ion-to-atom line intensity ratios, were lower for Sn and Hg (6500–7200 K) than those from Fe and Mg lines (7000–7800 K). The Sn II/Sn I and Hg II/Hg I, Fe II/Fe I, and Mg II/Mg I intensity ratios and the electron densities (n_e) were dependent on experimental conditions of plasma generation. Experimental and theoretically calculated ionization degrees were compared.

1. Introduction

Inductively coupled plasma (ICP) generated at atmospheric pressure has been recognized as a one of the most commonly applied techniques for both analytical purposes and spectrochemical investigations, including diagnostic studies. It has become attractive for simultaneous determination of several elements in a great variety of samples, namely, environmental, industrial, geological, biological, clinical, and food materials [1–3]. Additionally, although the method requires as a rule the liquid samples for measurements, the ability of hyphenation of the ICP with electrothermal vaporization or laser ablation allows analysis of the samples in their solid state [4, 5]. On the other hand, plasma discharge appears as an interesting tool enabling us to get knowledge and to understand the processes occurring in the plasma source [6–9].

Typically, solutions are introduced into the plasma by means of pneumatic (PN) or ultrasonic nebulization(USN), while chemical vapour generation (CVG) based on the reduction of the element ions with $NaBH_4$ in acidic medium has been widely employed to derivate elements into the form of volatile hydrides (e.g., As, Bi, Sb, Se, and Sn) or into cold vapours (Hg, Cd) [3, 10]. Systems without phase separation, that is, allowing the simultaneous introduction of volatile species and sample aerosol using pneumatic nebulization, can also be used to determine both hydride and nonhydride elements [3, 11–13].

Experimental conditions have effects on ICP parameters, for example, electron density (n_e), plasma temperatures (T_{exc}, T_{ion}, and T_{gas}), or plasma robustness employing the ion-to-atom intensity ratios (M II/M I). For the latter, the Mg II 280.3/Mg I 285.2 nm intensity ratio is usually considered.

Determination of n_e is commonly carried out using the H_β line profile. Excitation temperature is typically derived from atomic iron lines and the OH A-X 0-0 band serves usually for gas plasma temperature measurements. A number of papers have been devoted to ICP spectral diagnostics; however, nebulization systems have been predominantly investigated [6–9, 14–16] in comparison to the reports concerning CVG [11, 17–19]. In the case of PN, the effect of hydrogen in addition to the argon or combined effect with a desolvation step was also discussed [19–21].

Studies analysing the influence of CVG, PN, and combined PN + CVG systems on ICP characteristic are relatively rare and not consisted. Grotti et al. [18] investigated effect of operating conditions (power, carrier gas flow, and HCl and $NaBH_4$ concentrations) on T_{exc}, n_e, and Pb II/Pb I ratio in an axially viewed ICP coupled with pneumatic nebulization and ultrasonic nebulization associated with desolvation and with chemical vapour generation. At robust conditions and the CVG system, the electron number density was about 8% higher than at the PN system. Batistoni et al. [19] determined n_e and the H excitation temperature for the plasma with hydrogen from acidic $NaBH_4$ hydrolysis and compared obtained values with those determined for PN and dry plasma. The increase in n_e during $NaBH_4$ hydrolysis with reference to the dry plasma and PN was about 50% and 40%, respectively [19]. In the other work [17], the n_e values were above 70% higher at the CVG system than for dry plasma. Recently, spectroscopic and analytical characteristics of ICP with hydride generation with or without simultaneous introduction of the sample aerosol were presented by Pohl and Broekaert [11]. In this paper, the T_{ex} values determined from Ar I, Au I, Bi I, and Fe I were found to be close together for the sample introduction systems studied although differences for particular species were noted. The highest n_e values were obtained for the combined PN and CVG system while the n_e values at CVG and PN mode were comparable [11].

In the last years, attention has been paid to the use of other than H_β hydrogen lines for the electron density determination [19, 22–32] in various plasma. Konjević et al. [23] discussed difficulties appearing during experimental line profile analysis for higher members of Balmer series and compared theory versus experiments for low n_e plasma diagnostics. Mijatović et al. [24] tested the applicability of the H_γ line as a diagnostic tool at moderately low plasma densities using a low-pressure pulsed arc operating in a H_2:He gas mixture as a plasma source. Nikiforov et al. [29] discussed applications of Stark broadening hydrogenated (and nonhydrogenated) atomic lines for determination of n_e in atmospheric pressure plasma and presented equations for n_e estimation based on measured broadening of hydrogen Balmer series (H_α, H_β, and H_γ). For helium atmospheric pressure microwave induced plasma, the similar values of the electron density were obtained from the H_β and H_δ lines [28]. Recently, many works are devoted to determination of n_e from various hydrogen lines in laser-induced plasma [27, 30–32] due to very dynamic expansion and applications of such plasma. Pardini et al. [27] evaluated the plasma electron density through the measurements of the Stark broadening of the first-five members of the hydrogen Balmer series and compared experimental results with the predictions of three theories that described laser-induced breakdown plasma. The electron densities calculated from various H lines (with the exception of H_α) were comparable. The other works on laser-induced plasma diagnostics concern mainly exploration of the first-two Balmer series lines. For ICP only Batistoni et al. [19] measured the electron density in Ar-ICP for PN, CVG, and dry plasma by means of H_δ and H_γ lines and the results obtained from the two lines were not consisted.

The objective of the present study was determination and comparison of spectroscopic parameters of the inductively coupled plasma operating with pneumatic nebulization (aerosol), chemical vapour generation (gas mixture), and pneumatic nebulization combined with CVG. For the electron density determination, the usage of the first-four hydrogen lines of the Balmer series was tested. Atomic and ionic lines of Fe, Mg, Sn, and Hg served as thermometric species. In considerations, effects of sample introduction systems and related to the water, hydrogen, and mixture of hydrogen and water loading into the plasma were analysed. In addition, influence of the matrix of HCl and CH_3COOH on spectroscopic parameters was examined.

2. Materials and Methods

2.1. Instrumentation. All measurements were performed with the use of a Jobin Yvon sequential ICP-OES spectrometer (JY 38S) with a 1 m Czerny-Turner monochromator and two holographic gratings (4320 and 2400 grooves/mm). Spectra were recorded at the resolution of 0.01 nm in a sequential mode. Additionally, the image system for quick data acquisition in the range of 190–780 nm was used. Working parameters for the ICP-OES measurements are given in Table 1. The recorded line intensities were background corrected and expressed as net signals. The mean values from three repeated measurements were used in all investigations. The precision of the signal measurements expressed as the relative standard deviation (RSD) ranged, depending on the experimental conditions, from 1 to 6%.

2.2. Sample Introduction Systems. The ICP spectrometer, equipped with a modified cyclonic spray chamber and a parallel pneumatic nebulizer (Burgener), allowed nebulizing solutions (PN) as well as attaining chemical vapour generation (CVG) both separately and simultaneously with sample aerosol (PN + CVG). Solutions containing Sn(II), Hg(II), Mg(II), and Fe(II) at concentrations in the range of 5–50 $\mu g\,mL^{-1}$ were used. The solutions were acidified to final concentration of 1 $mol\,L^{-1}$ with HCl or CH_3COOH (HAc). In the case of phase separation (the CVG system only), volatile species of mercury and tin (vapours and hydrides) were generated in a continuous flow system. In the manifold applied, an acidified sample and reductant ($NaBH_4$) solutions were continuously pumped in two separate streams to Y-junction where they mixed and the CVG reaction occurred. Then, through 5 cm reaction coil, the reaction mixture was introduced at the bottom of the chamber (acting as a gas-liquid phase separator). Volatile species and other gaseous

Table 1: ICP operating parameters.

Generator	40.68 MHz
Monochromator	1 m with 4320/2400 grooves/mm grating
	Photomultipliers Hamamatsu R106 and R955
Rf power	1000 W and 1200 W
Injector i.d.	2.5 mm
Observation zone	12 mm above load coil
Ar flow rates:	
plasma gas	13–15 L min^{-1}
sheath gas	0.2 L min^{-1}
carrier gas	0.3 L min^{-1}
Solution uptake:	
acidified sample	1.0 mL min^{-1}
reductant	1.0 mL min^{-1}
Line wavelength (nm)	Sn II (189.9), Sn I (235.5), Hg II (194.2), Hg I (253.6), Mg II (280.3), Mg I (285.2), H_α (656.3), H_β (486.1) H_γ (434.0), and H_δ (410.2)
	Lines of Fe I (356–388 nm range) and Fe II (258–276 nm range)
Chemical vapour generation condition	
$NaBH_4$ concentration	0.75% (m/V) in 0.25 mol L^{-1} NaOH
HCl or CH_3COOH concentration	1.0 mol L^{-1}

by-products (mainly hydrogen) were swept by the stream of argon introduced through nebulizer and carried to the plasma torch. Conditions of the CVG mode are shown in Table 1.

For the simultaneous chemical vapour generation and pneumatic nebulization (the PN + CVG system), the acidified sample solution was aspirated into the chamber by pneumatic nebulizer and the $NaBH_4$ solution was introduced at the bottom of the chamber. Larger aerosol droplets deposited on the wall of the chamber dropped down to the bottom, where they reacted with incoming $NaBH_4$. Formed gaseous products as well as the sample aerosol were carried by a stream of the nebulizer argon into the plasma.

2.3. Plasma Parameters Calculations. The electron density was determined from Stark broadening of the H_α, H_β, and H_γ lines using tables obtained by computer simulation technique [33] assuming the electron temperature equal to 7500 K and a reduced mass of the emitter-perturber pair $\mu = 1$. Additionally, for the H_δ line, Griem's approximation [34, 35] was also applied.

For the extraction of the Stark broadening components from experimentally measured half widths of the hydrogen lines, the procedure described in work [26] and considering Doppler broadening and instrumental broadening was employed. The van der Waals and resonance broadening effects could be omitted. The instrumental line width was evaluated with the aid of the Ar lines lying in a neighbourhood of the hydrogen lines. The broadening caused by Doppler effect was calculated using common known expression at the assumption of the gas kinetic temperature equal to 4000 K. In the deconvolution, the GRAMS software and mixed Gaussian + Lorentz algorithm were used.

Spectroscopic temperatures and ionization degree were calculated at an assumption of partial thermal equilibrium. Ionization temperatures (T_{ion}) were calculated from the slope of the linearized form of the Saha-Boltzmann distribution [16, 36]:

$$\ln\left(\frac{I_i g_a A_a \lambda_i}{I_a g_i A_i \lambda_a}\right) = -\frac{E_{\text{ion}} + E_i - E_a}{kT} + \ln\left(\frac{2\left(2\pi m_e kT\right)^{3/2}}{n_e h^3}\right), \quad (1)$$

where I is the line intensity, g is the statistical weight, A is the transition probability, λ is the line wavelength, E is the energy of the upper state, E_{ion} is the first ionization potential, T is the ionization temperature, and n_e is the electron density. Subscripts "i" and "a" refer to ions and atoms, respectively.

At assumption of LTE, this method allows for the determination of the T_{ion} values independently of the n_e measurements. Plotting the $\ln(I_i g_a A_a \lambda_i / I_a g_i A_i \lambda_a)$ versus the energy sum $(E_{\text{ion}} + E_i - E_a)$ yields the straight line with the slope equal to $-1/kT_{\text{ion}}$. Ionization temperatures (T_{ion}) were calculated using fourteen atomic iron lines (Fe I) with excitation energies from 3.21 to 4.72 eV and fifteen ionic iron lines (Fe II) with excitation energies from 4.77 to 8.04 eV (Table 1). The Fe transition probabilities were taken from the NIST Atomic Spectra Database [37]. Additionally, the ionization temperatures were calculated using two-line method [36, 38] and the Mg II/Mg I, Hg II/Hg I, and Sn II/Sn I intensity ratios. The Hg, Sn, and Mg line transition probabilities were taken from the Kurucz database [39].

The ionization degrees (α_{ion}) were determined from the Saha ionization equation at assumption of plasma equilibrium:

$$K_j(T) = \frac{n_e N^+}{N} = 2\frac{(2\pi m_e kT)^{3/2}}{h^3}\frac{U^+(T)}{U(T)}\exp\left(-\frac{E_{\text{ion}} - \Delta E_{\text{ion}}}{kT}\right), \quad (2)$$

where $K_j(T)$ is equilibrium constant, N, N^+, and n_e are number of atoms, ions, and electrons, respectively, $U^+(T)$ and $U(T)$ are partition functions for atom and ion of the elements, and ΔE_{ion} is lowering of the ionization energy due to effect of the plasma on atoms and ions. In ICP, a contribution of multiple charged ions is negligible and hence α_{ion} may be determined using (2) as

$$\alpha_{\text{ion}A^+} = \frac{N_{A^+}}{N_A + N_{A^+}} = \frac{N_{A^+}/N_A}{1 + N_{A^+}/N_A}. \quad (3)$$

The partition functions for the atom and ion of the Mg, Fe, Sn, and Hg species were calculated from Irwin tables [40].

3. Results and Discussion

For the studied sample introduction systems emission spectra of Sn, Hg, H, Ar, Mg, OH, and CN were recorded while Fe lines were observed only if the PN and PN + CVG systems were used. At the condition of CVG in this study, intensities of the Fe lines were too low for reliable measurements, although the formation of volatile Fe compounds in the reaction with $NaBH_4$ was indicated [41, 42]. Unlike Sn and Hg that both easily form volatile species in the reaction with $NaBH_4$, the signals derived from Mg at the CVG mode were observed due to the transport of a fine aerosol [17].

At PN and PN + CVG modes, the Mg II/Mg I ratio was 8.5–9.0 and 10-11 for 1000 W and 1200 W, respectively, showing that the plasma was in robust conditions. During chemical vapour generation, the ratio increased to about 10.5 (1000 W) and 13 (1200 W) probably due to higher energy of plasma without water aerosol. The ratio was slightly higher with CH_3COOH than with HCl; however, these differences were in the standard deviation uncertainties.

3.1. Electron Density. The electron density was determined using hydrogen lines of the Balmer series. The H line profiles (both maximum intensities and half widths) depended significantly on the sample introduction system. All the H_α, H_β, H_γ, and H_δ lines were observed here with a sufficiently high intensity to be exactly measured. The H_β line intensities shown in Figure 1 well illustrate high sensitivity of H lines to changes in the plasma composition.

The contributions of H_2 originating from $NaBH_4$ hydrolysis (CVG) at the assumption of 100% efficiency of the reaction and from water dissociation (PN) were about 0.8 mmol/min and 1.0 mmol/min, respectively. The H line intensities at PN and CVG were close together and were approximately two times lower than it was observed for the mixture of the aerosol and products of chemical vapour generation (the combined PN + CVG system).

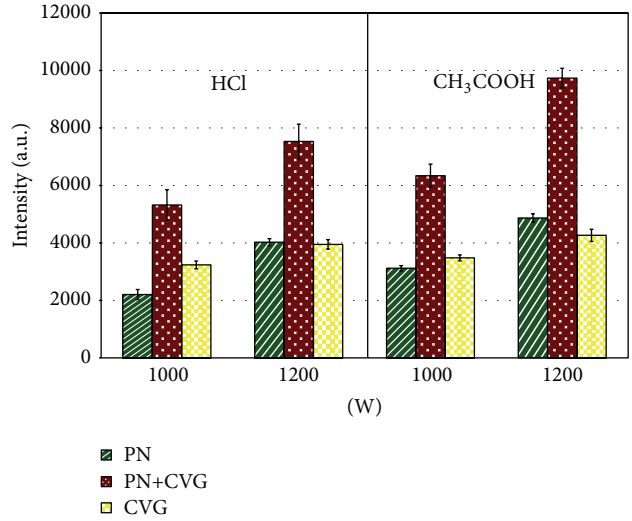

Figure 1: The H_β line intensities for various sample introduction systems.

At PN and at PN + CVG, the H line intensities were higher with the use of CH_3COOH than HCl by about 20–30%, while, for the system with CVG only, the effect of the acid was not essential (differences within the SDs). It confirms the role of a presence of the CH_3COOH matrix and H_2 in the plasma. With an increase in the rf power, the H signals were nearly 40, 30, and 20% higher for PN, PN + CVG, and CVG systems, respectively, independently of the kind of acid.

In plasma of moderately low electron density, the higher members of the Balmer series could be very useful for n_e determination since they are not self-absorbed and are considerably more Stark broadened [23, 24]. This means that the contribution of the Stark effect to overall broadening is significantly more pronounced in the case of H_γ and H_δ than in the case of H_α and H_β. Consequently, instrumental broadening and Doppler broadening contribute less to the H_γ and H_δ overall widths, what decreases an error in the Stark originated broadening measurements. In our spectra, the following relationship between experimental values of the full width at half maximum, FWHM ($\Delta\lambda_{1/2}$), was observed: $H_\alpha : H_\beta : H_\gamma : H_\delta = 1.0 : 2.9 : 4.4 : 6.0$. The H_ε line is often overlapped by the wing of a very intensive Ca II line at 396.8 nm. Taking into account that ICP serves mainly for analysis of water solutions with detectable Ca concentration even in the deionized water, the H_ε line was excluded and not considered. Hence, n_e was evaluated based on the H_α, H_β, H_γ, and H_δ lines. Because the tables given in [33] concern only first-three lines of Balmer series, for estimation of n_e from H_δ, broadening Griem's approximation [34, 35] was applied. The n_e values obtained from the H_α, H_β, H_γ, and H_δ lines at loading chemical vapour generation products into plasma are presented in Figure 2.

A very good agreement was observed between the n_e values derived from the H_β, H_γ, and H_δ lines; the same was observed for all systems. The n_e results based on H_γ were quite

Table 2: Electron densities ($n_e/10^{15}$ cm^{-3}) with their standard deviations ($n = 3$).

Matrix	PN		PN + CVG		CVG	
	1000 W	1200 W	1000 W	1200 W	1000 W	1200 W
HCl	0.69 ± 0.03	1.05 ± 0.02	0.72 ± 0.01	1.09 ± 0.03	1.08 ± 0.02	1.27 ± 0.04
CH_3COOH	0.56 ± 0.02	1.07 ± 0.03	0.63 ± 0.04	1.10 ± 0.01	1.09 ± 0.03	1.32 ± 0.06

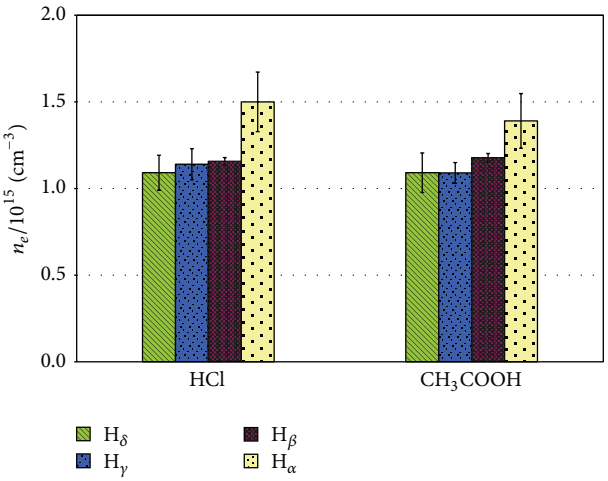

Figure 2: Values of n_e derived from various H lines (CVG).

well consistent with the values obtained from the H_β and H_δ lines, despite overlapping of the H_γ line at the wings by three relatively intense Ar I lines at 433.36, 433.53, and 434.52 nm, which can distort the H_γ line profile. Application of Griem's approximation led to slightly higher values (about 13%) of n_e when the H_β line was considered and the results obtained using H_β and H_δ were close together.

The H_α line is the narrowest ($\Delta\lambda_{1/2} \sim 0.08$–$0.09$ nm), only a few times broader than argon lines ($\Delta\lambda_{1/2} \sim 0.02$ nm) and with the relatively high contribution of the Doppler broadening ($\Delta\lambda_{1/2} \sim 0.03$ nm). The use of the H_α line led to the overestimation of n_e (up to 35%) in reference to the other H lines.

It may result from high contribution of other broadening effects [23, 29, 43] which are missed in calculations of the n_e values from H_α in an approach typical for atmospheric pressure argon plasma and not based on sophisticated procedure applied for example, for laser plasma.

If we take into account an effect of the van der Waals broadening and we employed the Voigt function for line profile [22], the electron density from the H_α line for the CVG mode and HCl was equal to $1.14 \cdot 10^{15}$ cm^{-3} what was in an agreement with the values obtained from the other hydrogen lines.

Nevertheless, FWHM of H_α is a few times smaller than FWHMs of the next hydrogen lines in the Balmer series, so uncertainty of n_e measurements from the H_α line is much higher. What is more, the H_α line is lying far from typical analytical range (200–460 nm) used for trace element determination by ICP-OES.

In spite of a large number of papers devoted to usage of higher members of hydrogen Balmer series lines, it is difficult to find a comparison between the n_e values experimentally determined from Stark broadening of different H lines. The electron density in Ar-ICP derived from the H_δ line by Batistoni et al. [19] was about twofold higher than the value calculated from the H_γ line. The authors suggested also spectral interferences in the case of the H_δ line (with nitrogen lines) but any interferences for H_γ were noted. In our opinion, in the case of Ar-ICP only the results obtained using H_α seem to be not reliable. This line could be useful for diagnostics of higher electron density plasma provided insignificant contribution of self-absorption and considering ion dynamic effects [32].

The electron density values based on the broadening of the H_β line for studied sample introduction systems are listed in Table 2. At the power of 1000 and 1200 W, the following relation was observed: $n_e(\text{PN}) \leq n_e(\text{PN + CVG}) < n_e(\text{CVG})$. It indicates that the addition of H_2 to the wet plasma (the PN + CVG system) does not change the n_e values, in practice. Some authors reported that at nonrobust conditions even a small amount of H_2 added to a sheathing or carrier gas resulted in an increase in n_e while at robust conditions such effect of hydrogen addition for dry plasma was found [20, 44]. It confirms our results. For the CVG system, n_e was about 40% (1000 W) and 20% (1200 W) higher than in the case of the PN and PN + CVG systems. Slightly higher n_e values were noted at the power of 1000 W for the PN and PN + CVG systems, in the presence of HCl than CH_3COOH. With an increase in power, the n_e values were comparable in the limits of standard deviation uncertainties for both acids.

Our previous work indicated [16] that for plasma loaded by a low solvent amount (more dried plasma), the electron number density was reduced. Similar effects were observed for Ar, He, and Ar + He microwave plasma—the electron number density was evidently higher for wet plasma (solution nebulization) [45]. It may be concluded that the increase in n_e is mainly related to a much better thermal conductivity of the dry plasma with hydrogen than the plasma loaded with water.

3.2. Ionization Temperatures and Degrees. The ionization temperatures obtained using (1) were calculated from Fe, Mg, Sn, and Hg ion-to-atom line intensity ratios and were presented for various experimental conditions in Figure 3.

Generally, the ionization temperatures did not show any significant changes with the experimental conditions and for all elements slightly increased with power (up to about 10%).

At lower power, the highest ionization temperatures were observed if only the gas mixture generated by chemical reaction with $NaBH_4$ (CVG) was introduced to plasma.

At higher power, the T_{ion} values were comparable if the CVG products or the mixture of the aerosol and CVG

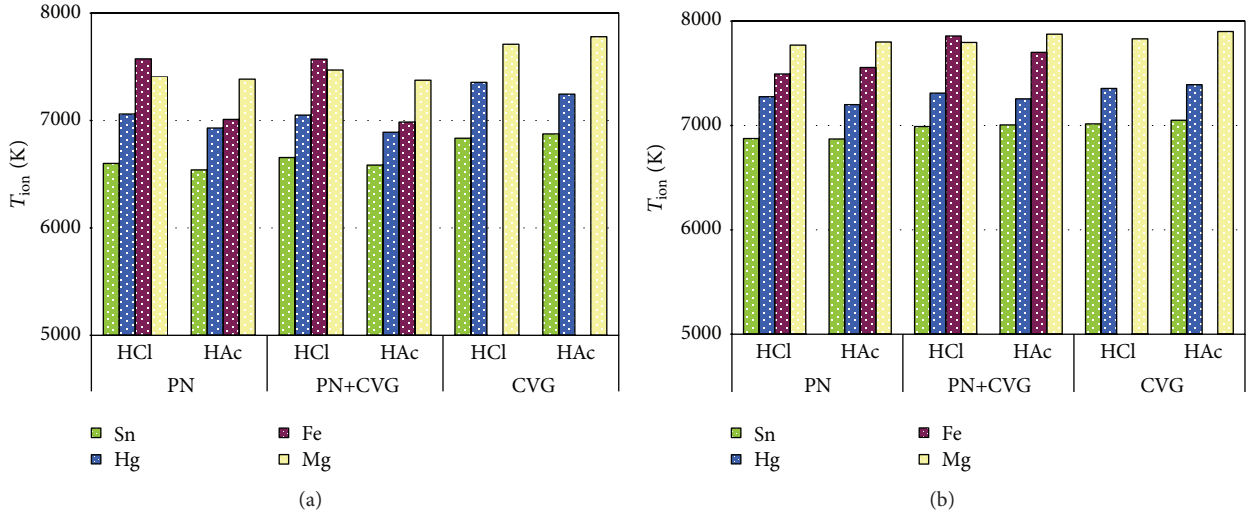

Figure 3: Ionization temperatures derived from the Sn, Hg, Fe, and Mg ion-to-atom intensity ratios measured at 1000 W (a) and 1200 W (b).

products (PN + CVG) was supplied into plasma and higher than those found in the case of aerosol introduction (PN).

At lower power, if aerosol was loaded to plasma (PN and PN + CVG), a weak influence of matrix on the ionization temperature was observed. For such conditions, the T_{ion} values were higher up to 700 K when HCl instead of CH_3COOH was employed. It confirms that introduction of acetic acid to the plasma at relatively low power results in decrease of plasma energy. An increase of power (for PN and PN + CVG) caused that the differences in T_{ion} values for both acids were insignificant. The Hg and Sn ionization temperatures were lower (by about 800–1800 K) than those from the Fe and Mg line intensity ratios. Generally, the changes in T_{ion} along with plasma conditions showed the same tendency as it was noted for the n_e values. However, the ionization temperature was found to be considerably less sensitive plasma parameter than the electron density.

The atomic (Fe I) and ionic (Fe II) excitation temperatures determined from (3) varied from 5400 to 6300 K and from 7100 to 8000 K, respectively, and showed similar changes with experimental conditions as those observed for the ionization temperatures. The ionization temperatures were higher than the Fe I temperatures and lower than the Fe II temperatures.

Investigation of the H_α, H_β, H_γ, and H_δ lines emitted by ICP indicated that their intensities did not correspond to the Boltzmann distributions. The excitation temperatures obtained from the H_γ and H_δ lines were from 4500 to 5500 K. So generally the LTE or pLTE conditions were not accomplished for H atoms, while it was observed for heavy atoms and ions present in atmospheric argon pressure ICP. The kinetic (plasma gas) temperature evaluated by comparison of simulated and experimental rotational intensity distribution measured from the $A^2\Pi$ - $X^2\Sigma^+$ 0-0 band of the OH spectrum was between 3500 K and 4000 K.

In addition to the temperatures, the ionization degrees were determined experimentally and theoretically. The calculations were performed from the Saha formulae (equation (1)), under assumption that T_e is comparable to T_{ion} and

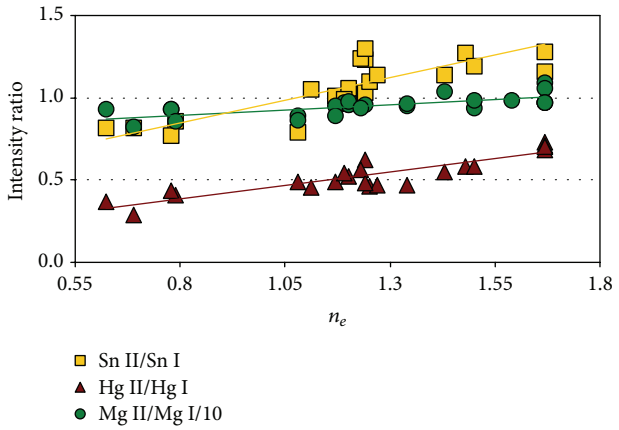

Figure 4: The ion-to-atom intensity ratio for Sn, Hg (left axis), and Mg (right axis) versus the electron density (in 10^{15} cm^{-3}).

equal to 8000 K. The very satisfactory agreement between experimental ionization degrees (from M II/M I ratios) and theoretically calculated ones was observed for Fe and Mg (the differences did not exceed 2%) but for Sn and Hg the experimental α_{ion} values (78% and 20%) were lower than the ionization degrees from the Saha formula (86% and 30%). The α_{ion} and T_{ion} values suggest that populations of atom and ion levels of Sn and Hg are much far from thermodynamic equilibrium than it takes a place in the case of Mg and Fe.

The ion-to-atom intensity ratios measured from Sn, Hg, and Mg lines were plotted against the n_e values determined at various experimental conditions (see Figure 4). The correlation coefficients R for Hg, Sn, and, Mg were calculated to be 0.9, 0.8, and 0.7, respectively. The slope coefficients for Sn and Hg (0.55 and 0.33, resp.) were considerably higher than that for Mg (0.13). It means the ion-to-atom intensity ratios measured here from Sn and Hg lines were significantly more sensitive to changes in plasma characteristics and conditions than the Mg II/Mg I ratio.

4. Conclusions

Spectroscopic investigations of the most prominent hydrogen lines belonging to the Balmer series in point of view their application for determination of electron density in Ar-ICP were carried out. The H_β, H_γ, and H_δ lines were suitable for accurate measurements of the Stark broadening effect and appropriate for determination of n_e. The n_e values obtained from the H_γ and H_δ line were in a very good agreement with those from the H_β line at the all experimental conditions, while n_e from the H_α line was significantly higher. It indicates that both the H_γ and H_δ line profiles can be alternatively used for electron density measurements. However, if the effect of the van der Waals broadening was taken into account and the Voigt function was used for line profile fitting, the agreement between the electron density from the H_α and from the other hydrogen lines could be achieved.

The electron density was found to be the plasma parameter sensitive and reacting for changes in experimental conditions. For the dry plasma supplied by hydrogen, the n_e values were higher by a factor of 1.2–1.9 in dependence of the power than those obtained at pneumatic nebulization. In the case of mixed gas-liquid system, the plasma parameters are comparable to those observed for pneumatic nebulization.

The ionization temperatures determined from Fe, Mg, Sn, and Hg were different and not too much sensitive for variation of experimental conditions. The following dependence was observed for the temperatures derived from Fe I and Fe II lines:

$$T_{\text{exc}}\,(\text{Fe I}) < T_{\text{ion}}\,(\text{Fe}) \leq T_{\text{exc}}\,(\text{Fe II})\,. \tag{4}$$

Intensity distributions of the H_α, H_β, H_γ, and H_δ lines were not in a satisfactory agreement with the Boltzmann distributions characteristic for LTE or pLTE conditions. The plasma gas temperature evaluated from rotational line intensities of the OH A-X 0-0 spectrum was between 3500 K and 4000 K.

At lower power, the plasma was less resistant to matrix effects and an influence of hydrogen. The Fe, Mg, Sn, and Hg ion-to-atom intensity ratios were observed to be dependent on experimental conditions. The correlation plots between the M II/M I ratios and n_e could be quite well approximated by linear equations and the R coefficients were 0.9, 0.8, and 0.7 for Hg II/Hg I, Sn II/Sn I, and Mg II/Mg I, respectively. The Hg II/Hg I and Sn II/Sn I ratios were more sensitive for n_e changes than the Mg II/Mg I ratio.

Competing Interests

The authors declare that they have no competing interests.

Acknowledgments

This work was financed by a statutory activity subsidy from the Polish Ministry of Science and Higher Education for the Faculty of Chemistry of Wroclaw University of Technology.

References

[1] R. K. Soodan, Y. B. Pakade, A. Nagpal, and J. K. Katnoria, "Analytical techniques for estimation of heavy metals in soil ecosystem: a tabulated review," *Talanta*, vol. 125, pp. 405–410, 2014.

[2] R. Sańchez, J. L. Todolí, C.-P. Lienemann, and J.-M. Mermet, "Determination of trace elements in petroleum products by inductively coupled plasma techniques: a critical review," *Spectrochimica Acta Part B: Atomic Spectroscopy*, vol. 88, pp. 104–126, 2013.

[3] P. Pohl and R. E. Sturgeon, "Simultaneous determination of hydride- and non-hydride-forming elements by inductively coupled plasma optical emission spectrometry," *Trends in Analytical Chemistry*, vol. 29, no. 11, pp. 1376–1389, 2010.

[4] M. Resano, F. Vanhaecke, and M. T. C. de Loos-Vollebregt, "Electrothermal vaporization for sample introduction in atomic absorption, atomic emission and plasma mass spectrometry—a critical review with focus on solid sampling and slurry analysis," *Journal of Analytical Atomic Spectrometry*, vol. 23, no. 11, pp. 1450–1475, 2008.

[5] M. S. Gomes, E. R. Schenk, D. Santos Jr., F. J. Krug, and J. R. Almirall, "Laser ablation inductively coupled plasma optical emission spectrometry for analysis of pellets of plant materials," *Spectrochimica Acta B*, vol. 94-95, pp. 27–33, 2014.

[6] D. Goitom, E. Björn, W. Frech, and M. T. C. de Loos-Vollebregt, "Radial ICP characteristics for ICP-AES using direct injection or microconcentric nebulisation," *Journal of Analytical Atomic Spectrometry*, vol. 20, no. 7, pp. 645–651, 2005.

[7] J. R. Dettman and J. W. Olesik, "Reduction of matrix effects in quantitative and semi-quantitative inductively coupled plasma-optical emission spectrometry using a partial local thermodynamic equilibrium model and an internal standard," *Spectrochimica Acta Part B: Atomic Spectroscopy*, vol. 76, pp. 96–108, 2012.

[8] H. Lindner, A. Murtazin, S. Groh, K. Niemax, and A. Bogaerts, "Simulation and experimental studies on plasma temperature, flow velocity, and injector diameter effects for an inductively coupled plasma," *Analytical Chemistry*, vol. 83, no. 24, pp. 9260–9266, 2011.

[9] E. Tognoni, M. Hidalgo, A. Canals et al., "Combination of the ionic-to-atomic line intensity ratios from two test elements for the diagnostic of plasma temperature and electron number density in Inductively Coupled Plasma Atomic Emission Spectroscopy," *Spectrochimica Acta Part B: Atomic Spectroscopy*, vol. 62, no. 5, pp. 435–443, 2007.

[10] M. Ślachciński, "Recent achievements in sample introduction systems for use in chemical vapor generation plasma optical emission and mass spectrometry: from macro- to microanalytics," *Applied Spectroscopy Reviews*, vol. 49, no. 4, pp. 271–321, 2014.

[11] P. Pohl and J. A. C. Broekaert, "Spectroscopic and analytical characteristics of an inductively coupled argon plasma combined with hydride generation with or without simultaneous introduction of the sample aerosol for optical emission spectrometry," *Analytical and Bioanalytical Chemistry*, vol. 398, no. 1, pp. 537–545, 2010.

[12] L. R. Gómez, G. D. Márquez, and J. R. Chirinos, "Dual nebulizer sample introduction system for simultaneous determination of volatile elemental hydrides and other elements," *Analytical and Bioanalytical Chemistry*, vol. 386, no. 1, pp. 188–195, 2006.

[13] Z. Benzo, M. N. Matos-Reyes, M. L. Cervera, and M. de la Guardiaa, "Simultaneous determination of hydride and non-hydride forming elements by inductively coupled plasma optical emission spectrometry," *Journal of the Brazilian Chemical Society*, vol. 22, no. 9, pp. 1782–1787, 2011.

[14] A. Klostermeier, C. Engelhard, S. Evers, M. Sperling, and W. Buscher, "New torch design for inductively coupled plasma optical emission spectrometry with minimised gas consumption," *Journal of Analytical Atomic Spectrometry*, vol. 20, no. 4, pp. 308–314, 2005.

[15] C. Engelhard, G. C.-Y. Chan, G. Gamez, W. Buscher, and G. M. Hieftje, "Plasma diagnostic on a low-flow plasma for inductively coupled plasma optical emission spectrometry," *Spectrochimica Acta Part B: Atomic Spectroscopy*, vol. 63, no. 6, pp. 619–629, 2008.

[16] J. Borkowska-Burnecka, A. Leśniewicz, and W. Zyrnicki, "Comparison of pneumatic and ultrasonic nebulizations in inductively coupled plasma atomic emission spectrometry—matrix effects and plasma parameters," *Spectrochimica Acta Part B: Atomic Spectroscopy*, vol. 61, no. 5, pp. 579–587, 2006.

[17] M. Wełna and W. Żyrnicki, "Influence of chemical vapor generation conditions on spectroscopic and analytical characteristics of a hyphenated CVG-ICP system," *Journal of Analytical Atomic Spectrometry*, vol. 24, no. 6, pp. 832–836, 2009.

[18] M. Grotti, C. Lagomarsino, and J. M. Mermet, "Effect of operating conditions on excitation temperature and electron number density in axially-viewed ICP-OES with introduction of vapours or aerosols," *Journal of Analytical Atomic Spectrometry*, vol. 21, no. 9, pp. 963–969, 2006.

[19] D. A. Batistoni, R. N. Garavaglia, and R. E. Rodríguez, "Evaluation of hydrogen line emission and argon plasma electron concentrations resulting from the gaseous sample injection involved in hydride generation-ICP-atomic emission spectrometric analysis," *Fresenius' Journal of Analytical Chemistry*, vol. 366, no. 3, pp. 221–227, 2000.

[20] M. Murillo, R. Amaro, and A. Fernández, "Influence of hydrogen gas over the interference of acids in inductively coupled plasma atomic emission spectrometry," *Talanta*, vol. 60, no. 6, pp. 1171–1176, 2003.

[21] H. Wiltsche, F. Moradi, and G. Knapp, "Evaluation of the oscillator frequency of a free running RF generator as a diagnostic tool for inductively coupled plasma-optical emission spectrometry," *Spectrochimica Acta B*, vol. 71-72, pp. 48–53, 2012.

[22] E. A. Oks, *Stark Broadening of Hydrogen and Hydrogenlike Spectral Lines in Plasmas: The Physical Insight*, Alpha Science International, Oxford, UK, 2006.

[23] N. Konjević, M. Ivković, and N. Sakan, "Hydrogen Balmer lines for low electron number density plasma diagnostics," *Spectrochimica Acta—Part B: Atomic Spectroscopy*, vol. 76, pp. 16–26, 2012.

[24] Z. Mijatović, D. Nikolić, R. Kobilarov, and M. Ivković, "Stark broadening of the hydrogen H_γ spectral line at moderately low plasma electron densities," *Journal of Quantitative Spectroscopy and Radiative Transfer*, vol. 111, no. 7-8, pp. 990–996, 2010.

[25] A. Qayyum, R. Ahmad, S. A. Ghauri, A. Waheed, and M. Zakaullah, "Hydrogen Balmer-β and Balmer-γ emission profiles in an abnormal glow region of hydrogen plasma," *Vacuum*, vol. 80, no. 6, pp. 574–580, 2006.

[26] J. Torres, J. M. Palomares, A. Sola, J. J. A. M. Van Der Mullen, and A. Gamero, "A Stark broadening method to determine simultaneously the electron temperature and density in high-pressure microwave plasmas," *Journal of Physics D: Applied Physics*, vol. 40, no. 19, pp. 5929–5936, 2007.

[27] L. Pardini, S. Legnaioli, G. Lorenzetti et al., "On the determination of plasma electron number density from Stark broadened hydrogen Balmer series lines in Laser-Induced Breakdown Spectroscopy experiments," *Spectrochimica Acta Part B: Atomic Spectroscopy*, vol. 88, pp. 98–103, 2013.

[28] M. Ivković, S. Jovićević, and N. Konjević, "Low electron density diagnostics: development of optical emission spectroscopic techniques and some applications to microwave induced plasmas," *Spectrochimica Acta Part B: Atomic Spectroscopy*, vol. 59, no. 5, pp. 591–605, 2004.

[29] A. Yu. Nikiforov, Ch. Leys, M. A. Gonzalez, and J. L. Walsh, "Electron density measurement in atmospheric pressure plasma jets: stark broadening of hydrogenated and non-hydrogenated lines," *Plasma Sources Science and Technology*, vol. 24, no. 3, Article ID 034001, 18 pages, 2015.

[30] C. G. Parigger, "Atomic and molecular emissions in laser-induced breakdown spectroscopy," *Spectrochimica Acta Part B: Atomic Spectroscopy*, vol. 79-80, pp. 4–16, 2013.

[31] L. D. Swafford and C. G. Parigger, "Laser-induced plasma spectroscopy of hydrogen Balmer series in laboratory air," *Applied Spectroscopy*, vol. 68, no. 9, pp. 1016–1020, 2014.

[32] C. Aragón and J. A. Aguilera, "Determination of the local electron number density in laser-induced plasmas by stark-broadened profiles of spectral lines: comparative results from H_α, Fe I and Si II lines," *Spectrochimica Acta Part B: Atomic Spectroscopy*, vol. 65, no. 5, pp. 395–400, 2010.

[33] M. A. Gigosos and V. Cardeñoso, "New plasma diagnosis tables of hydrogen Stark broadening including ion dynamics," *Journal of Physics B: Atomic, Molecular and Optical Physics*, vol. 29, no. 20, pp. 4795–4838, 1996.

[34] H. R. Griem, *Spectral Line Broadening by Plasmas*, Academic Press, New York, NY, USA, 1974.

[35] P. Kepple and H. R. Griem, "Improved stark profile calculations for the hydrogen lines Hα, Hβ, Hγ, and Hδ," *Physical Review*, vol. 173, no. 1, pp. 317–325, 1968.

[36] C. Aragón and J. A. Aguilera, "Characterization of laser induced plasmas by optical emission spectroscopy: a review of experiments and methods," *Spectrochimica Acta Part B: Atomic Spectroscopy*, vol. 63, no. 9, pp. 893–916, 2008.

[37] NIST Atomic Line Database, http://physics.nist.gov/PhysRefData/Handbook.

[38] M. M. Rahman and M. W. Blades, "Atmospheric pressure, radio frequency, parallel plate capacitively coupled plasma-excitation temperatures and analytical figures of merit," *Spectrochimica Acta B*, vol. 52, no. 13, pp. 1983–1993, 1997.

[39] Kurucz Atomic Spectroscopic Database, http://www.pmp.uni-hannover.de/cgi-bin/ssi/test/kurucz/sekur.html.

[40] A. W. Irwin, "Polynomial partition function approximations of 344 atomic and molecular species," *The Astrophysical Journal Supplement Series*, vol. 45, pp. 621–631, 1981.

[41] M. Wełna, J. Lasowska, and W. Zyrnicki, "Determination of some inorganic species of Fe, Mn and Cr by chemical vapor generation hyphenated with inductively coupled plasma atomic emission spectrometry," *Journal of the Brazilian Chemical Society*, vol. 22, no. 6, pp. 1164–1169, 2011.

[42] P. Pohl and W. Żyrnicki, "On the transport of some metals into inductively coupled plasma during hydride generation process," *Analytica Chimica Acta*, vol. 429, no. 1, pp. 135–143, 2001.

[43] J. M. Luque, M. D. Calzada, and M. Sáez, "Experimental research into the influence of ion dynamics when measuring the electron density from the Stark broadening of the Hα and Hβ lines," *Journal of Physics B: Atomic, Molecular and Optical Physics*, vol. 36, no. 8, pp. 1573–1584, 2003.

[44] I. Novotny, J. C. Farinas, J.-L. Wan, E. Poussel, and J.-M. Mermet, "Effect of power and carrier gas flow rate on the tolerance to water loading in inductively coupled plasma atomic emission spectrometry," *Spectrochimica Acta Part B: Atomic Spectroscopy*, vol. 51, no. 12, pp. 1517–1526, 1996.

[45] K. Jankowski and A. Jackowska, "Spectroscopic diagnostics for evaluation of the analytical potential of argon + helium microwave-induced plasma with solution nebulization," *Journal of Analytical Atomic Spectrometry*, vol. 22, no. 9, pp. 1076–1082, 2007.